atmosphere

MDPI

Article

"On-Line" Heating Emissions Based on WRF Meteorology—Application and Evaluation of a Modeling System over Greece

Natalia Liora [1,*], Serafim Kontos [1], Daphne Parliari [1], Dimitris Akritidis [2], Anastasia Poupkou [3], Dimitris K. Papanastasiou [4] and Dimitrios Melas [1]

[1] Laboratory of Atmospheric Physics, Department of Physics, Aristotle University of Thessaloniki, 54124 Thessaloniki, Greece; mkontos@auth.gr (S.K.); dparliar@auth.gr (D.P.); melas@auth.gr (D.M.)
[2] Department of Meteorology and Climatology, School of Geology, Aristotle University of Thessaloniki, 54124 Thessaloniki, Greece; dakritid@geo.auth.gr
[3] Academy of Athens, Research Centre for Atmospheric Physics and Climatology, Solonos 84, 10680 Athens, Greece; apoupkou@academyofathens.gr
[4] Department of Environmental Sciences, Campus Geopolis, University of Thessaly, 41110 Larissa, Greece; dkpapan@uth.gr
* Correspondence: lioranat@auth.gr

Abstract: The main objective of the present study is the development of an "on-line" heating emissions modeling system based on simulated meteorological data and its integration with air quality modeling systems in order to improve their accuracy. The WRF-CAMx air quality modeling system is applied over Greece for the cold period of 2015 (January–April, October–December) for two emissions scenarios: using the (a) "on-line" heating emissions based on WRF meteorology and (b) "static" heating emissions based on static temporal profiles. The monthly variation in total "on-line" heating emissions followed the temporal pattern of the air temperature over Greece, leading to the highest heating emissions in January and February, while higher differences in emissions between winter and spring/autumn months were identified in comparison with the static ones. The overall evaluation of the WRF-CAMx modeling system using the "on-line" heating emissions revealed satisfactory model performance for the mean daily air quality levels. The comparison between the simulated and observed mean monthly concentrations revealed an improvement in the pattern of mean monthly concentrations for the "on-line" scenario. Higher values of the index of agreement and correlation for the mean daily values were also identified for the "on-line" scenario in most monitoring sites.

Keywords: air pollution; on-line heating emissions; WRF; CAMx; evaluation; Greece

check for updates

Citation: Liora, N.; Kontos, S.; Parliari, D.; Akritidis, D.; Poupkou, A.; Papanastasiou, D.K.; Melas, D. "On-Line" Heating Emissions Based on WRF Meteorology—Application and Evaluation of a Modeling System over Greece. *Atmosphere* **2022**, *13*, 568. https://doi.org/10.3390/atmos13040568

Academic Editor: Roberto Bellasio

Received: 1 March 2022
Accepted: 30 March 2022
Published: 31 March 2022

Publisher's Note: MDPI stays neutral with regard to jurisdictional claims in published maps and institutional affiliations.

Copyright: © 2022 by the authors. Licensee MDPI, Basel, Switzerland. This article is an open access article distributed under the terms and conditions of the Creative Commons Attribution (CC BY) license (https://creativecommons.org/licenses/by/4.0/).

1. Introduction

Air pollution in urban centers is a significant environmental problem that leads to adverse effects on human health. According to the EEA [1], in 2015 in Greece, 12,000 premature deaths were linked to exposure to particulate matter (PM). Road transport, residential heating and industry are some of the main anthropogenic activities that deteriorate the air quality levels in urban centers [2–4], while the EEA [1] showed that residential heating was the major contributor to PM10, PM2.5 and CO emissions in Europe in 2016. Several studies in the past have examined the impacts of heating emissions on human health [5–7], including effects on respiratory and cardiovascular health.

At this point, it is worth mentioning that the financial crisis that broke out in Greece in 2009 has resulted in a shift in the fuel used for heating (mainly residential) from conventional fuels (i.e., oil) to biomass (mainly wood), leading to increased air pollution mainly in urban centers [8–11]. Sariggianis et al. [7] identified a significant increase in particle concentration levels during the cold period of 2012 compared to 2011, in Thessaloniki, Greece, attributed to biomass burning for residential heating.

It is of the utmost importance to develop accurate emissions inventories related to residential and commercial heating integrated with air quality modeling systems in order to ensure the validity of the simulated results for the adoption of the appropriate mitigation measures for the improvement of air quality in cities and human health. Most emissions methodologies for the estimation of heating emissions found in the literature are based on static temporal profiles taken by European databases [2,9,12,13] or based on monthly fuel consumption data according to the date of purchase of fuel (i.e., for oil or wood/biomass), leading to an inaccurate temporal distribution of heating emissions. The use of heating systems is directly associated with the meteorological conditions and therefore static temporal profiles result in high uncertainties in the estimations of heating pollutant emissions. Thus, there is the necessity for estimating heating emissions more accurately, taking into account the changes in meteorological conditions.

For this reason, the current study aims to develop a validated "on-line" heating emissions modeling system based on the calculated Heating Degree Days (HDD) from the hourly meteorological simulated data of the meteorological model, the Weather Research and Forecasting Model (WRF v4.1.2 [14]). The concept of the methodology is to develop potential emissions data (i.e., mean daily potential pollutant emission data per HDD) that can be representative for past or close future years since it has been considered that the ratio of fuel consumption data per HDD in a region remains constant. Thus, the calculated daily gridded emissions data based on the simulated HDD of a past or close future study year will be proportional to the simulated air temperature data of the corresponding study year. Moreover, mean daily potential emission data per HDD on a horizontal spatial level over Greece (6×6 km^2) or Thessaloniki (2×2 km^2) can be provided to the scientific community since they can be used by any air quality modeling system for air quality studies or for operational air quality modeling systems. These data are based on mean annual consumption data for three consecutive past years, as well as annual historical statistical data of HDD over Greece. It should be noted that the main aim of the paper is not to address climate change, in which the far-future socioeconomic development is crucial in addition to temperature increases. The heating emissions presented fit the purposes of air quality monitoring with shorter reference time periods with respect to the longer climate change perspective. Finally, the heating emissions modeling system is integrated with an air quality modeling system that has been previously implemented in many air quality studies for European cities [15–21] and the Middle East [22,23]. However, major updates have been done concerning mainly the anthropogenic emissions estimations over Greece (see Section 2.2).

In the current study, the "on-line" heating emissions modeling system is integrated with an air quality modeling system to be implemented and evaluated over high-resolution domains over Greece for the year 2015. Section 2 presents the air quality modeling system implemented and the methodologies used for the estimation of the anthropogenic emission inventory focusing on the on-line heating emissions. Section 3 presents the temporal and spatial distribution of the calculated heating emissions. The modeling simulation scenarios implemented and the ground-based measurement data used for the evaluation of the modeling system are also presented. The evaluation of the on-line heating emissions modeling system, as well of the meteorological fields driving them, is presented through the comparison of the simulated air pollutants' concentration data with the observed ones for two simulated scenarios (i.e., "on-line" and "static" heating emissions scenarios). Section 4 summarizes the major outcomes of the study.

2. Materials and Methods

2.1. Modeling Application

An air quality modeling system consisting of the meteorological model, the Weather Research and Forecasting Model (WRF v4.1.2; [14]), and the three-dimensional Comprehensive Air Quality Model with extensions (CAMx v.6.4; [24]) has been applied over three two-way nesting domains: a coarse grid with 18×18 km^2 horizontal resolution that

covered Europe, North Africa and Middle East (d01), a 6 × 6 km^2 horizontal resolution grid that covered the Mediterranean Region (d02) and a 2 × 2 km^2 horizontal resolution grid covering the greater area of Thessaloniki, Greece (d03) (Figure 1) for the year 2015. Emissions results will be shown only for domain d02 (6 × 6 km^2), which covers Greece. Each domain has 35 unevenly spaced full sigma layers in the vertical direction with the model top defined at 100 hPa. For the initialization of WRF, the various surface/upper-level atmospheric and land–soil variables taken from the European Centre for Medium-Range Weather Forecasts (ECMWF, [25]) at 3 h temporal and 0.75° spatial resolution have been used. The chemical initial and boundary conditions from Copernicus Atmosphere Monitoring Service Information (CAMS) [26] have been used for the application of CAMx.

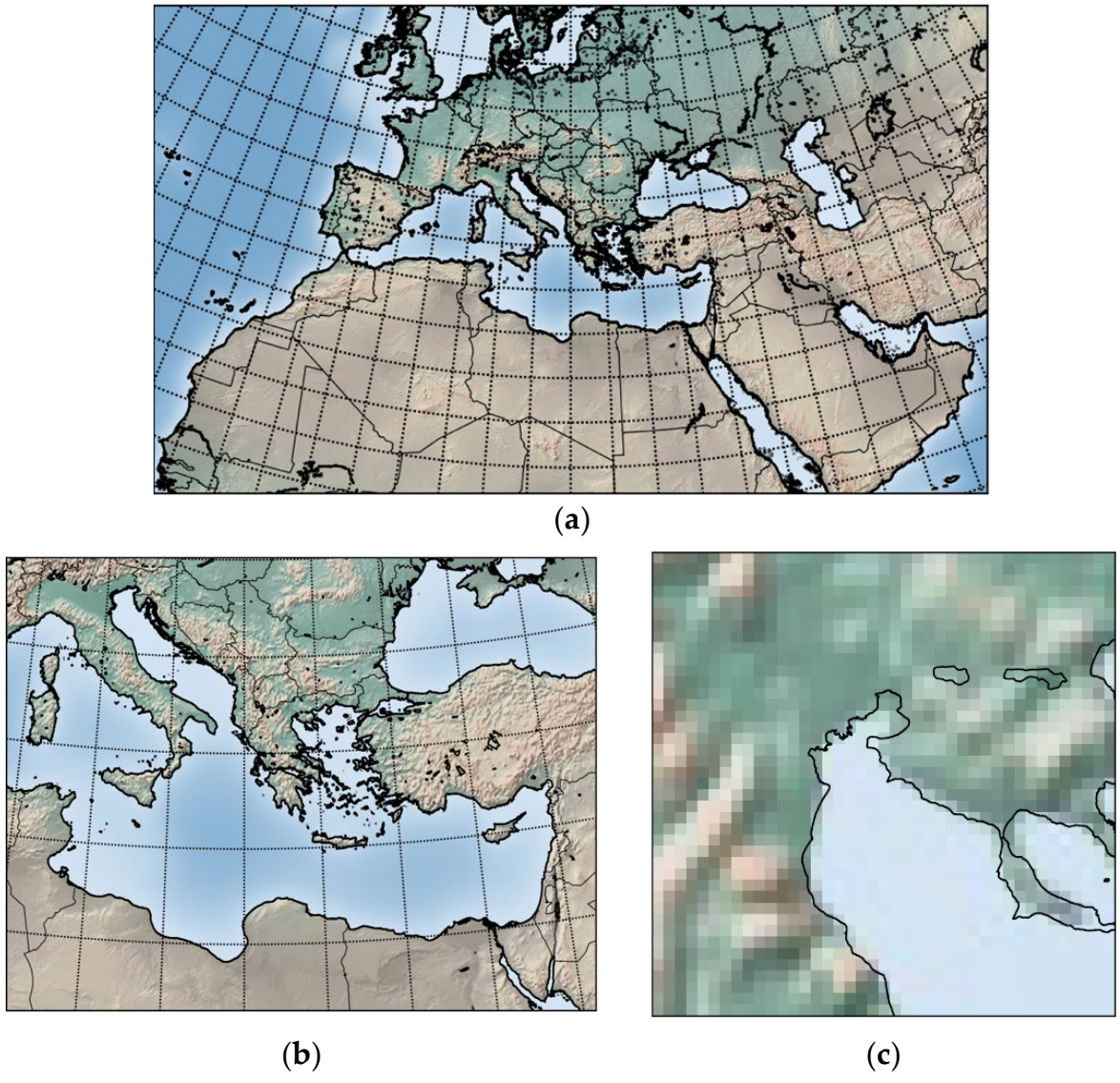


Figure 1. Modeling domains: (**a**) Europe, North Africa and Middle East (18 × 18 km^2, d01), (**b**) Eastern Mediterranean (6 × 6 km^2, d02) and (**c**) greater area of Thessaloniki (2 × 2 km^2, d03).

Anthropogenic emissions have been estimated for the following pollutants: carbon monoxide (CO), nitrogen oxides (NO_x), non-methane volatile organic compounds (NMVOC), ammonia (NH_3), sulfur dioxide (SO_2) and particulate matter (PM10 and PM2.5). The anthropogenic emissions over Greece used in the simulations are presented in detail in Section 2.2. For the other European countries, in the modeling domains, the anthropogenic emissions database of CAMS Regional European Emissions version 2 (CAMS-

REGv.2.2.1; [27]) for the year 2015 was used, which provides annual gridded pollutant emissions for each GNFR sector (i.e., aggregated sector 'gridded NFR') over a high-resolution European domain (0.1 × 0.05 degrees, ~6 × 6 km^2). The anthropogenic emissions database of EDGAR v.4.3.2 [28] for the year 2010 was used for the estimation of anthropogenic emissions over the non-European countries included in the modeling domains. The database has a resolution of 0.1 × 0.1 degree. The aforementioned emissions data were spatially, temporally (on a monthly, weekly and hourly basis) and chemically distributed over the two studied domains for each emission source using the temporal and chemical split factors (split factors are given on country level) provided by The Netherlands Organization (TNO), along with the CAMS-REG database, being representative for the year 2015. The chemical speciation was performed for NMVOCs into 23 species (alcohols, propane, butanes, etc.) and for PM into 5 species: elemental carbon (EC), organic carbon (OC), sodium (Na), sulfates (SO_4) and other minerals. For the spatial distribution of the emission data over the study domains, the open-source Geospatial Data Abstraction Library (GDAL; [29]) as well as the Climate Data Operators (CDO; [30]) tools have been used. Moreover, updated annual gridded (over the CAMS-REG domain) potential particle dust emissions from resuspension due to road traffic have been provided by TNO [31]. Anthropogenic dust emissions were spatially distributed over the study domains similarly to the emission data of the other databases, while they were temporally analyzed using the temporal profiles of the CAMS-REG database, taking also into account meteorological restrictions using the 2015 hourly WRF meteorological data, i.e., dust emissions were forced to zero during precipitation events.

Natural emissions from windblown dust, sea salt and vegetation (i.e., biogenic emissions) have been estimated with the Natural Emissions Model (NEMO, [18,22]) using the hourly meteorological data of WRF.

2.2. Emissions Inventory for Greece

In the current study, an anthropogenic emissions inventory over Greece for the year 2015 has been developed for the following pollutants—CO, NO_x, SO_2, NMVOCs, NH_3, PM10 and PM2.5—using either a bottom-up methodology (i.e., based on regional or national activity data) or the CAMS-REGv.2.2.1 anthropogenic emissions database.

A bottom-up methodology has been implemented in order to estimate air pollutant emissions over Greece from the following emissions sources: heating, fuel transformation, solvent use, road transport, agriculture (fertilizer, field burning, manure management). For the rest of the emissions sources for which activity data were not available (i.e., energy, industrial sector, non-road transport and waste), the annual anthropogenic emission database of CAMS-REGv2.2.1 [27] for the year 2015 has been used as described in Section 2.1. Their spatial distribution over the study domains was performed similarly to the methodology described in Section 2.1.

The most updated methodologies of the EMEP/EEA Air Pollutant Emission Inventory Guidebook 2016 [32] have been used for the estimation of the annual air pollutant emissions from heating, fuel transformation, solvent use and agriculture, while the emission model COPERT v.5.2.2 [33] was implemented for the emissions estimations from road transport. In the following, a description of the input data and methodologies used for each emission source is presented. The current study focuses on the study and evaluation of the on-line heating emissions modeling system and therefore a detailed description is provided for this source.

2.2.1. Heating

Heating emissions have been estimated using the Tier II methodology of the EMEP/EEA Emission Inventory Guidebook 2016 [32] based on the annual fuel consumption of gas oil, natural gas and biomass burning (only for wood). For the estimations of biomass burning emissions (only for biomass), the Tier I methodology of EMEP/EEA 2016 was implemented.

The final pollutant emissions were estimated separately for biomass burning and other fuels (i.e., gas oil, natural gas).

The activity data used for heating emissions calculations are the following:

- The mean annual fuel consumption of gas oil and natural gas for each Greek prefecture for the period 2015–2017, which have been derived from the Hellenic Statistical Authority and the Hellenic Gas Transmission System Operator (www.desfa.gr, accessed on 1 February 2019), respectively.
- The mean annual residential consumption of wood and biomass for the period 2015–2016 on a national level, which has been provided by the Center for Renewable Energy Sources and Saving (www.cres.gr, accessed on 1 February 2019) for the estimation of biomass burning emissions. In addition, concerning the type of technology/practice used for biomass burning, it was assumed that 66% of households use fireplaces and 34% woodstoves [9].

Annual heating emissions have been initially estimated on a prefectural scale over Greece. Given the fact that biomass burning consumption data were given on a national scale, the spatial disaggregation of the biomass burning data was made on a prefectural level using the number of households per fuel type used for heating purposes for each Greek prefecture based on a survey conducted by the Hellenic Statistical Authority for 2011.

In the current study, heating emissions have been estimated for two scenarios using two different methodologies in terms of the temporal and spatial distribution:

- "On-line" heating emissions have been estimated based on annual statistical data of the Heating Degree Days (HDD) of Greek prefectures and using the hourly meteorological data derived from the application of the WRF model for the cold period (January–April and October–December) of 2015. In particular, the annual heating emissions per Greek prefecture were converted to mean daily heating emissions per degree day (°Cday) using statistical data of the mean annual HDD per Greek prefecture. Following this, a further spatial distribution on a municipality level was performed using population data on the municipality level (i.e., the number of households per fuel type used for heating purposes for each Greek municipality derived from the Hellenic Statistical Authority). The mean daily heating emissions per HDD from biomass burning and other sources for each municipality of Greece were spatially distributed on the 6×6 km^2 and 2×2 km^2 resolution grids. The potential mean daily emissions (g/°Cday) from biomass burning and other sources were firstly distributed on a weekly basis using temporal profiles. The final daily gridded pollutant emissions have been calculated based on the hourly meteorological data of the WRF model for the year 2015 and the hourly profiles. More specifically, the HDD for each simulated day of WRF and each grid cell has been estimated based on the hourly air temperature T_h and the reference temperature T_i used for the HDD estimations, which was defined at 18 °C [34] as follows:

$$HDD = \frac{1}{24} \sum_{k=1}^{24} (T_i - T_{h,k}) \quad (1)$$

The HDD and therefore hourly emissions have been estimated only when $T_i - T_{h,k} > 0$. The weekly and hourly profiles used for the temporal distribution of pollutant emissions from oil and natural gas (other sources) were provided by TNO, along with the emissions database of CAMS-REG v2.2.1. The distribution of heating emissions from biomass burning on a weekly and hourly basis has been assessed using the temporal profiles used in the study of Athanasopoulou et al. [8], which revealed a distinct diurnal variation in biomass burning, with higher concentrations of the wood burning fraction of black carbon in the evening as well as during weekends compared with the morning and weekdays, respectively, in the area of Athens, Greece. Similar diurnal variations in Athens had been also shown in other studies [4,35–37], while Saffari et al. [11] identified higher concentrations of wood smoke tracers in the evening period compared with the morning in Thessaloniki, Greece.

- Annual "static" heating emissions on a prefectural level have been spatially distributed over the 6 × 6 km^2 (Greece) and 2 × 2 km^2 (Thessaloniki) resolution grids using only population data on the municipality level (i.e., number of households per fuel type use for heating purposes for each Greek municipality derived from the Hellenic Statistical Authority). Static heating emissions from oil and natural gas (other sources) have been distributed monthly using only static monthly profiles derived by the database of CAMS-REG v2.2.1. The temporal distribution on a weekly and hourly basis was derived using the static temporal profiles of CAMS-REG v2.2.1 and Athanasopoulou et al. [8] for oil and natural gas (other sources) and biomass burning (wood/biomass) emissions, respectively.

2.2.2. Other Sources

The Tier I methodology of the EMEP/EEA Air Pollutant Emission Inventory Guidebook 2016 [32] has been used for the estimation of NMVOC emissions from fuel transformation using the annual amount of fuel sold per Greek prefecture in 2015 derived from the Hellenic Statistical Authority (EL.STAT). The Tier II methodology of the EMEP/EEA Air Pollutant Emission Inventory Guidebook 2016 [32] has been used for the estimation of NMVOC emissions from solvent use using the results of the Production and Sales of Manufacturing Products (PRODCOM) survey for 2015 [38] on a national level. Data include products such as pesticides, coatings and cosmetics. The spatial distribution of the annual emissions per Greek prefecture over the study domains was performed using population data on a municipality level [39].

Emissions from road transport over Greece have been estimated using the emission model COPERT v.5.2.2 [33], which calculates emissions from the road transport sector using the methodology of EMEP/EEA, including exhaust (covering hot- and cold-start exhaust emissions), fuel evaporation (from gasoline vehicles) and non-exhaust (tyre, break and surface wear) emissions from passenger cars, light-duty vehicles, heavy-duty vehicles, mopeds and motorcycles. COPERT v.5.2.2 was implemented on a national level for the urban and rural network using the annual COPERT data for Greece for the year 2015 [33]. For highways, activity data concerning the annual number of vehicles traveled over each highway (or for each part of the highway) and the length of the highway's network (or part of it) were used. The abovementioned calculated urban and rural national road transport emissions were spatially distributed over the urban centers and rural network, respectively, over the study domains also using population data on a municipality level [39].

Agricultural activities include fertilizers, field burning and manure management (livestock). Emissions from fertilizers have been estimated using the annual consumption of fertilizers in Greece for the year 2015, derived from the Hellenic Fertilizers' Association (S.P.E.L; www.spel.gr (accessed on 1 February 2019)), in combination with the total area of croplands per Greek prefecture taken by EL.STAT. The methodology for estimating agricultural crop residue burning emissions was based on the area of land on which crops are grown whose residues are burned (i.e., wheat, barley, maize, rice, peas, beans, rye, sugar) per Greek prefecture taken by EL.STAT for the year 2015. Emissions from manure management (i.e., livestock) have been estimated based on the number of animals by kind and Greek prefecture for the year 2016 according to a farm and manure holdings structure survey derived from EL.STAT. The Copernicus CORINE Land Cover (CLC) database v.18.5 with a spatial resolution of 250 m was used for the spatial distribution of agricultural emissions per Greek prefecture over the study domain (i.e., distributed over agricultural areas including pastures for manure management).

Finally, the annual emissions have been temporally distributed on a monthly, weekly and hourly basis using mainly the temporal profiles provided by TNO along with the CAMS-REG database for Greece. However, for selected sources, some temporal profiles were based on national surveys.

2.2.3. Chemical Distribution

The chemical speciation of NMVOCs (into 23 species) and PM (into 5 species; elemental carbon (EC), organic carbon (OC), sodium (Na), sulfates (SO_4) and other minerals) was performed for each emission source using the chemical split factors for Greece provided by TNO along with the emission database of CAMS-REGv2.2.1.

3. Results and Discussion

3.1. Evaluation of the Meteorological Model

WRF meteorological data for the cold period of the year 2015 (January to April and October to December) used in the current study have been evaluated through the comparison of the mean daily simulated data with ground-based measurements. The evaluation concerns the near-surface air temperature T (°C) at 2 m above ground level since this field is used in estimations of the "on-line" heating emissions. The ground-based measurement data for eight monitoring sites have been derived from the National Oceanic and Atmospheric Administration (https://www.noaa.gov, accessed on 1 February 2019), the national monitoring network of the National Observatory of Athens (available online at http://meteosearch.meteo.gr, accessed on 1 February 2019) and the Municipality of Thessaloniki. A detailed description of the main characteristics of each monitoring site is given in Table S1 of the Supplementary Materials. The simulated results of the WRF model concern the domain d02 (6×6 km^2) covering Greece.

Table 1 presents the statistical metrics for the daily mean air temperature over the eight monitoring sites during the cold period of 2015 (January–April, October–December). The statistical metrics estimated are the following: the mean bias (MB), the mean absolute error (MAE), the Pearson's correlation coefficient (R) and the Index of Agreement (IOA) (a definition is given in the Supplementary Materials). The statistical analysis was performed using the simulated data over the 6×6 km^2 domain.

Table 1. Statistical metrics for the near-surface air temperature for each monitoring site over the cold period of 2015 (January–April, October–December).

Site Name	MB (°C)	MAE (°C)	R	IOA
Egnatia	−1.27	1.67	0.94	0.95
Martiou	−0.38	1.27	0.95	0.97
Athinai	−0.61	1.12	0.96	0.97
Nea Smyrni	−0.84	1.10	0.97	0.97
Larissa	−1.07	1.59	0.94	0.96
Patras	−0.75	1.27	0.94	0.96
Ioannina	0.86	2.23	0.80	0.88
Heraklion, airport	0.90	1.16	0.96	0.96

The performance of the WRF model is found to be overall satisfactory, with an IOA higher than 0.95 for the majority of stations examined, where a slight underestimation is found. The largest mean absolute error (MAE) is found for Ioannina station (2.23 °C) and the lowest MAE for Nea Smyrni (1.1 °C). Figure 2 depicts the daily variation in the observed and simulated air temperature values, identifying very good agreement in the daily variability.

3.2. Heating Emissions in Greece

In this section, the heating emissions results estimated "on-line" with the use of the simulated HDD of WRF for the domain of Greece (d02, 6×6 km^2) are presented and discussed. They are also compared with the "static" emission data.

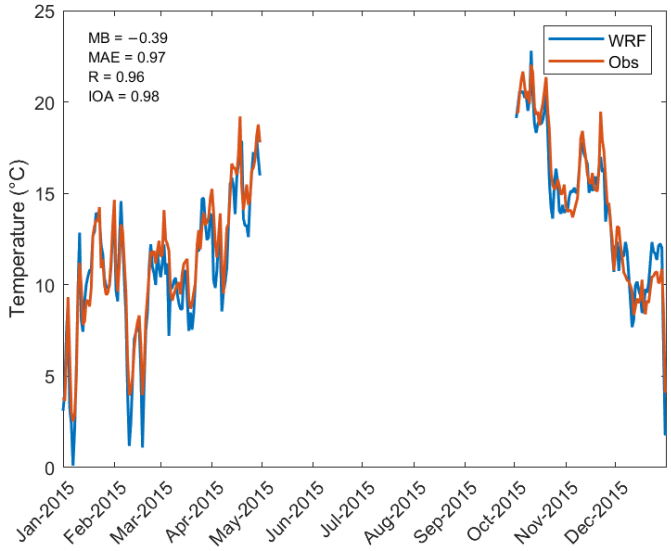


Figure 2. Observed and modeled time series of mean daily air temperature (°C) during the cold period of 2015, averaged over all stations.

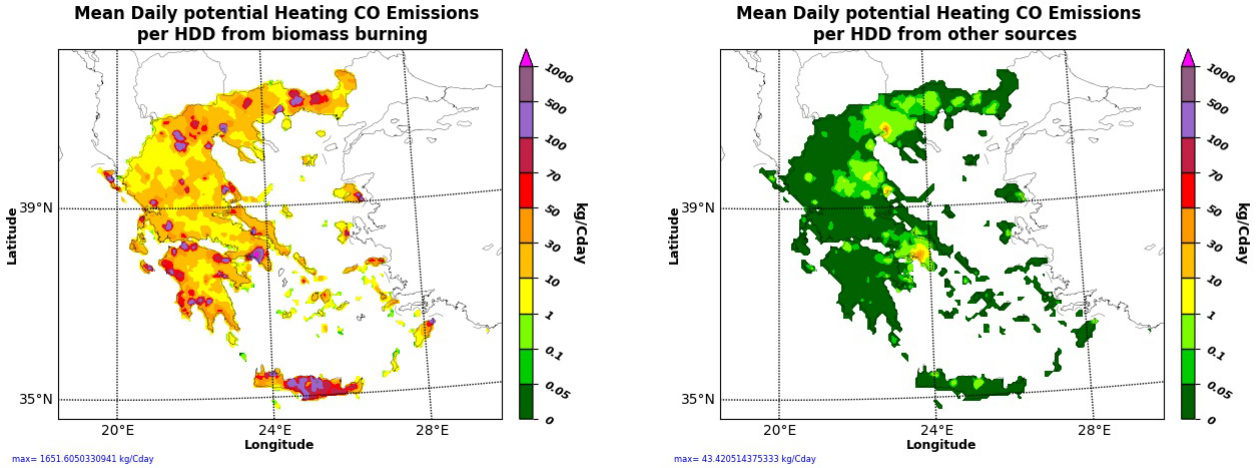
Figure 3 depicts the mean daily potential heating emissions of CO, NO_x and PM10 from biomass burning (wood, biomass) and other sources (natural gas, oil) over the grid cells (6×6 km^2) that cover the area of Greece as they have been estimated using the methodology described in Section 2.2.1. The daily potential emission data can be used only for the cold period of a year (i.e., January to April and October to December). It is shown that the potential daily heating emissions per HDD from conventional fuels (i.e., oil/natural gas) are highest mainly in the dense urban centers (i.e., Athens, Thessaloniki, Larissa, Volos). On the other hand, relatively high emissions per HDD from biomass burning are identified in rural areas of northern and western–southern Greece, attributed to the spatial distribution of energy use for heating in households per fuel type on a municipality level. PM2.5 presents a similar spatial distribution to PM10 emissions and therefore is not presented in Figure 3 (the same is true for SO_2, which presents a similar distribution to NO_x).

Using the aforementioned mean daily potential emissions data (Figure 3), the final "on-line" heating emissions have been estimated based on the calculated HDD from the hourly meteorological data of WRF for the cold period of 2015 (i.e., January to April and October to December).

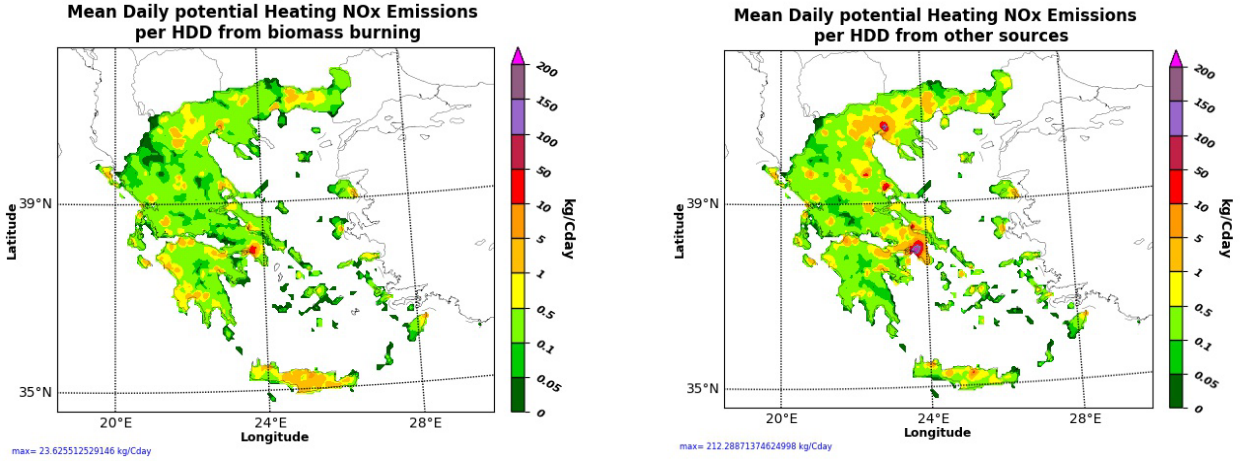
According to the total anthropogenic emissions estimations over Greece for the cold period of 2015, fuel combustion for heating is the major contributor to PM10 and PM2.5 emissions by 47% and 60%, respectively, while it is the second contributor to CO (19%) and NMVOC (22%) emissions, for which the industrial sector and solvent use are the major contributors, respectively. A lower share of heating emissions is attributed to NO_x, SO_2 and NH_3 (<10%). Finally, it is estimated that 163 ktn, 8.1 ktn, 3.3 ktn, 4 ktn, 26.4 ktn, 35 ktn and 31 ktn of CO, NO_x, SO_2, NH_3, NMVOCs, PM10 and PM2.5 are emitted over Greece from heating during the cold period of 2015.

Figure 4 illustrates the monthly variation in the total heating emissions over Greece, which present a distinct peak in January. Similar amounts of pollutants are emitted also in February, while emissions in March and December are slightly lower. It is worth mentioning that the static monthly profiles usually used in European emission inventories follow a different pattern, leading to lower differences in heating emissions between April, October and November and the winter months. For instance, on-line heating emissions in April are around −65% lower than those estimated in January, while the corresponding difference in static emissions is estimated to be approximately −30%. In Figure 5, the static monthly heating emissions based on the temporal profile derived from TNO for Greece are also

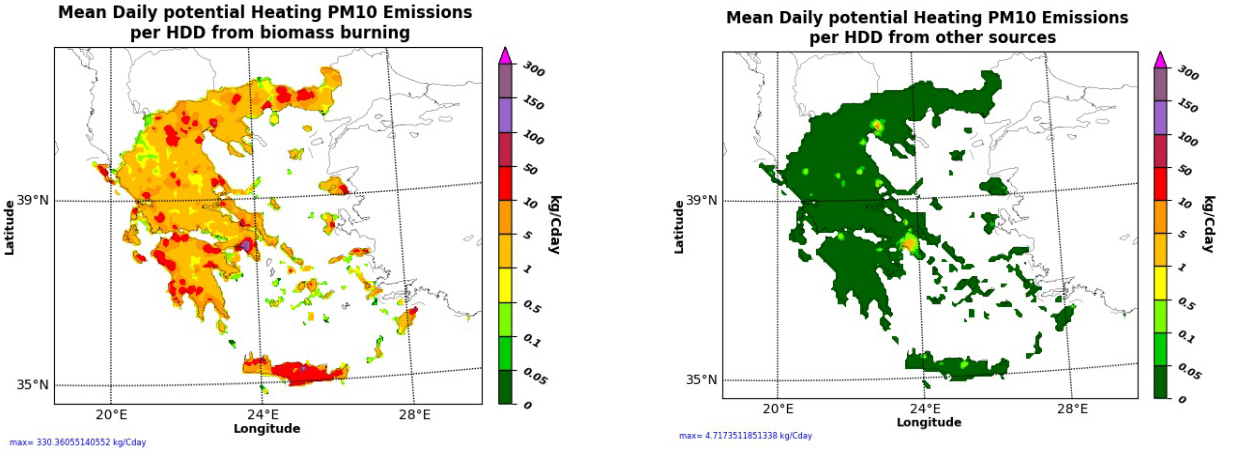
shown, highlighting the differences in the monthly variation in emissions between the two methodologies (i.e., static vs. on-line).



(**a**)



(**b**)



(**c**)

Figure 3. Spatial distribution of mean daily potential emissions per HDD (kg/Cday) of (**a**) CO, (**b**) NO_x and (**c**) PM10 from biomass burning (wood/biomass) (left) and other sources (oil, natural gas) (right) over Greece (6×6 km^2, d01).

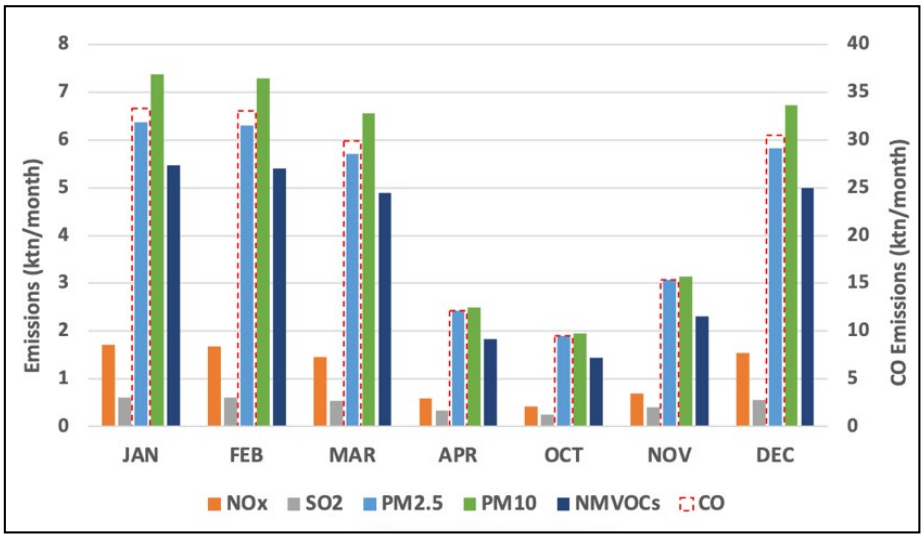


Figure 4. Monthly variation in total "on-line" heating emissions (in ktn/month) for NO_x, SO_2, PM2.5, PM10, NMVOCs and CO (secondary axis) over Greece for the cold period of 2015 (January–April, October–December).

Figure 6 presents the total monthly heating pollutant emissions from biomass burning (wood, biomass) and other sources (gas, oil) over the grid cells that cover the area of Greece for January, when heating emissions are maximum. CO and PM10 emissions from heating can reach up to 10 tn/km^2/month and 2 tn/km^2/month, respectively, in dense urban areas (i.e., Athens) due to wood combustion. NO_x emissions from other sources (oil, natural gas) are higher than those from wood combustion, taking their maximum values in Athens and Thessaloniki (>1 tn/km^2/month), while 100–500 kg/km^2/month of NO_x is emitted in smaller cities.

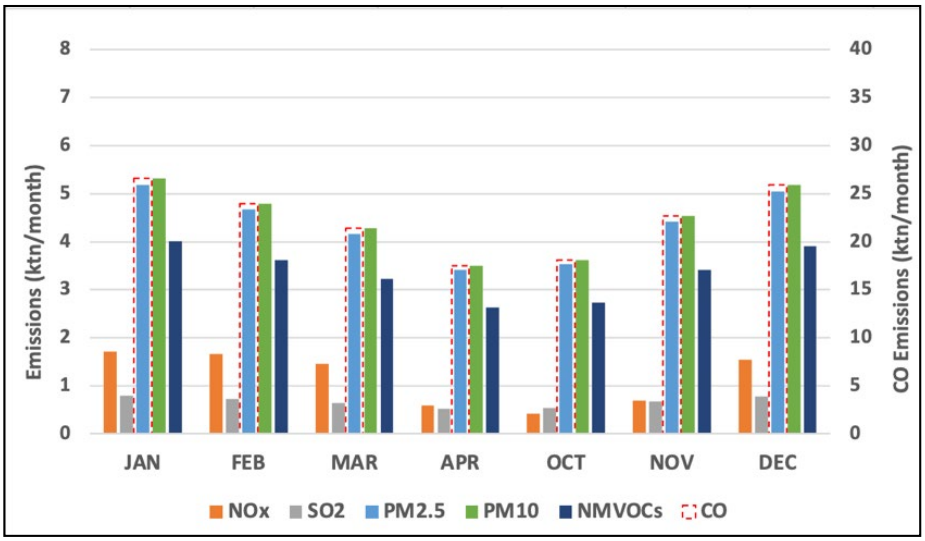
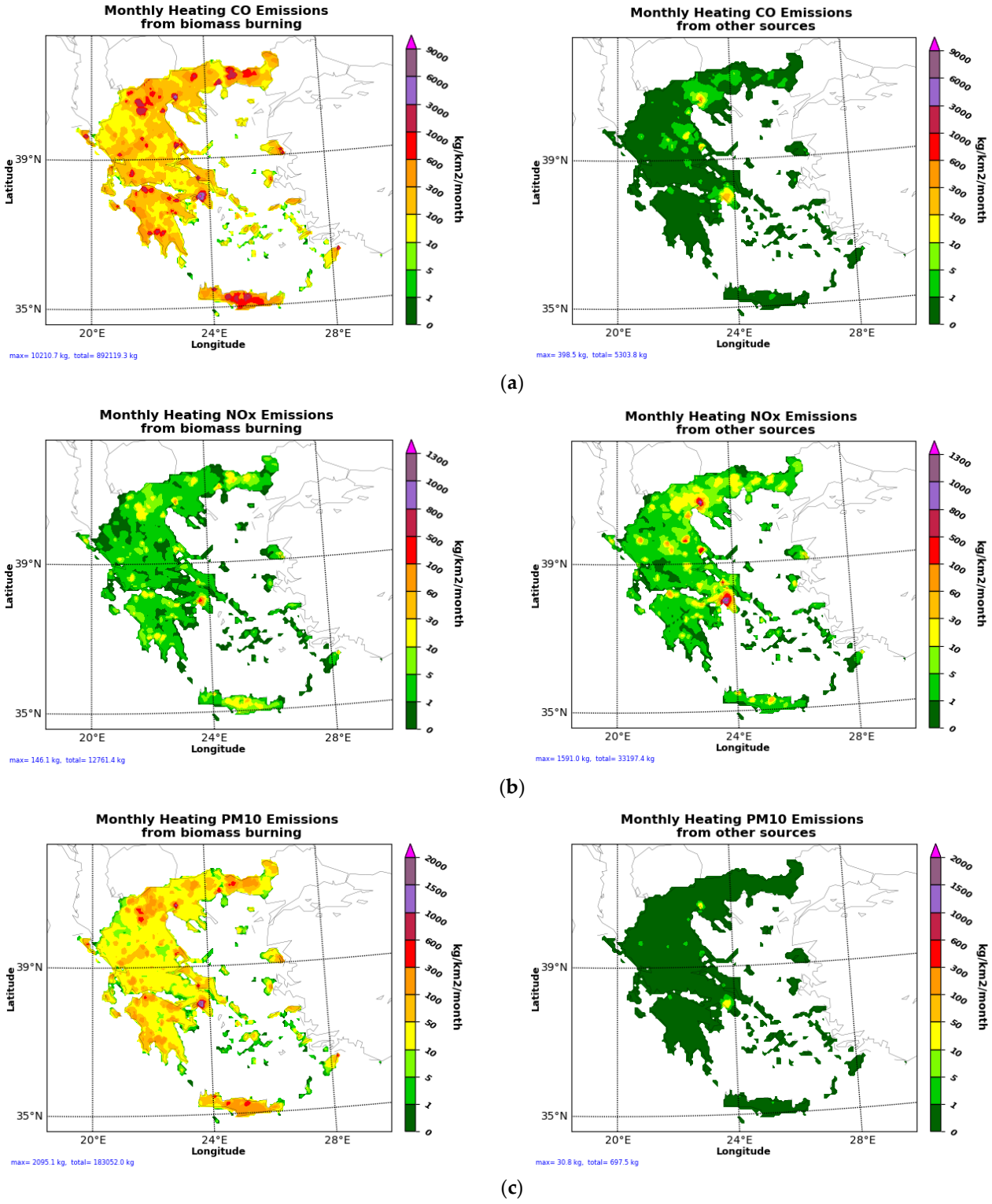


Figure 5. Monthly variation in total "static" heating emissions (in ktn/month) for NO_x, SO_2, PM2.5, PM10, NMVOCs and CO (secondary axis) over Greece for the cold period of 2015 (January–April, October–December).



(**a**)

(**b**)

(**c**)

Figure 6. Spatial distribution of total monthly emissions (kg/km^2) of (**a**) CO, (**b**) NO_x and (**c**) PM10 from biomass burning (wood/biomass) (left) and other sources (oil, natural gas) (left) over Greece (6×6 km^2 grid) for January 2015.

3.3. Evaluation of the Modeling System

In order to evaluate the "on-line" heating emissions produced with the WRF meteorology as described in Section 2.2, the WRF-CAMx modeling system is implemented for

two scenarios using the "on-line" and the "static" heating emissions, respectively, for the cold period of 2015 (January–April and October–December):

1. "On-line" heating emissions scenario (On-line SCN);
2. "Static" heating emissions scenario (Static SCN).

The evaluation of the WRF-CAMx air quality modeling system is performed through the comparison of the simulated air pollution data of the on-line SCN with ground-based measurement data of O_3, CO, NO, NO_2 and PM10. It should be mentioned that the statistical analysis for the Thessaloniki area has been performed using the simulated concentration data of the high-resolution domain (d03, 2 × 2 km^2). For the rest of the areas of Greece, simulated data over the 6 × 6 km^2 domain (over Greece) were used.

The statistical metrics (description is given in the Supplementary Materials) that are used for the quantitative evaluation of the results are the Pearson's correlation coefficient (R), the mean bias (MB), the ratio factor of 2 (Fac2) and the Index of Agreement (IOA), which is indicative of the overall performance.

Measurement data were taken from national networks (Table S2 in the Supplementary Materials) over Greece. For the area of Thessaloniki, additional air quality measurement data were derived from the monitoring network of the Municipality of Thessaloniki. The monitoring and recording of the measurements of the Municipal Network is systematic, on a 24 h basis. For the rest of Greece, measurements have been taken from the Ministry of the Environment and Energy of Greece, which provides ground-based measurements of pollution data on a daily or hourly basis from the monitoring networks of the Greek Regional Units. Finally, measurement data of Thissio station (Athens) have been derived from the National Observatory of Athens (NOA). The statistical analysis for the Athens area was performed for urban background stations excluding urban traffic stations due to the strong effect of road transport emissions on air quality levels, which cannot be accurately simulated by the photochemical model over the 6 × 6 km^2 domain (d02).

An analysis of the statistical measures between simulated and observed air pollutant concentrations for the on-line SCN is presented in order to identify the overall performance of the air quality modeling system. A comparison of the statistical measures of R and IOA between the two simulated scenarios, as well as a comparison between the observed mean monthly variation with the simulated ones of the two implemented scenarios, is presented for the evaluation of the "on-line" heating emissions modeling system.

Tables 2–7 present the statistical metrics for O_3, CO, NO_2, NO, PM10 and SO_2 mean daily concentrations for different monitoring sites over Greece for the on-line SCN for the cold period of 2015.

Table 2. Statistical metrics for O_3 mean daily concentrations ($\mu g/m^3$) for each monitoring site over Thessaloniki, Greece (for d03 domain, 2 × 2 km^2) and the rest of Greece (for d02 domain, 6 × 6 km^2) for the cold period of 2015 (January–April, October–December) for the on-line_SCN.

Site Name	Location in Greece	MB	Fac2	R	IOA
PER	Athens	−7.5	0.85	0.70	0.80
Thissio	Athens	−23.1	0.97	0.70	0.75
SMY	Athens	−12.3	0.79	0.52	0.68
LIO	Athens	−4.7	0.93	0.65	0.78
KOR	Athens	6.8	1.3	0.72	0.75
AGS	Thessaloniki	11.6	1.84	0.66	0.77
KOD	Thessaloniki	−2.6	1.07	0.60	0.76
Lagada	Thessaloniki	4.2	1.2	0.53	0.72
Martiou	Thessaloniki	5.0	1.3	0.65	0.79
Dimarxeio	Thessaloniki	10.8	1.5	0.66	0.72
Mean (Greece)		**−1.2**	**1.18**	**0.65**	**0.75**

Table 3. Statistical metrics for CO mean daily concentrations (mg/m^3) for each monitoring site over Thessaloniki, Greece (for d03 domain, 2 × 2 km^2) and the rest of Greece (for d02 domain, 6 × 6 km^2) for the cold period of 2015 (January–April, October–December) for the on-line_SCN.

Site Name	Location in Greece	MB	Fac2	R	IOA
PER	Athens	−0.27	0.72	0.60	0.51
Thissio	Athens	0.01	1.14	0.58	0.75
SMY	Athens	−0.22	0.87	0.54	0.59
KAL	Thessaloniki	−0.21	0.65	0.59	0.48
Mean (Greece)		**−0.17**	**0.85**	**0.58**	**0.58**

Table 4. Statistical metrics for NO_2 mean daily concentrations (μg/m^3) for each monitoring site over Thessaloniki, Greece (for d03 domain, 2 × 2 km^2) and the rest of Greece (for d02 domain, 6 × 6 km^2) for the cold period of 2015 (January–April, October–December) for the on-line_SCN.

Site Name	Location in Greece	MB	Fac2	R	IOA
PER	Athens	−2.1	1.04	0.36	0.62
Thissio	Athens	10.3	1.61	0.37	0.54
SMY	Athens	3.1	1.3	0.44	0.67
Lagada	Thessaloniki	−2.8	1.05	0.53	0.73
Martiou	Thessaloniki	−10.4	0.80	0.43	0.61
Dimarxeio	Thessaloniki	−13.9	0.69	0.49	0.58
Mean (Greece)		**−2.6**	**1.08**	**0.44**	**0.63**

Table 5. Statistical metrics for NO mean daily concentrations (μg/m^3) for each monitoring site over Thessaloniki, Greece (for d03 domain, 2 × 2 km^2) and the rest of Greece (for d02 domain, 6 × 6 km^2) for the cold period of 2015 (January–April, October–December) for the on-line_SCN.

Site Name	Location in Greece	MB	Fac2	R	IOA
PER	Athens	−4.7	1.26	0.60	0.62
Thissio	Athens	−4.1	1.80	0.79	0.80
SMY	Athens	−3.6	1.60	0.76	0.75
Lagada	Thessaloniki	−20.2	0.57	0.62	0.58
Martiou	Thessaloniki	−19.9	0.54	0.62	0.55
Dimarxeio	Thessaloniki	−16.5	0.62	0.67	0.58
Mean (Greece)		**−11.5**	**1.07**	**0.68**	**0.65**

Table 6. Statistical metrics for PM10 mean daily concentrations (μg/m^3) for each monitoring site over Thessaloniki, Greece (for d03 domain, 2 × 2 km^2) and the rest of Greece (for d02 domain, 6 × 6 km^2) for the cold period of 2015 (January–April, October–December) for the on-line SCN.

Site Name	Location in Greece	MB	Fac2	R	IOA
AGP	Athens	7.5	1.50	0.74	0.80
LYK	Athens	3.9	1.20	0.71	0.83
SMY	Athens	−0.6	1.06	0.72	0.85
Thissio	Athens	18.7	1.93	0.52	0.62
AGS	Thessaloniki	0.2	1.17	0.50	0.67
KOD	Thessaloniki	−5.5	1.10	0.43	0.60
Malakopi	Thessaloniki	−10.5	0.87	0.35	0.56
Martiou	Thessaloniki	−5.7	0.93	0.41	0.62

Table 6. *Cont.*

Site Name	Location in Greece	MB	Fac2	R	IOA
IOA	Ioannina	−23.6	0.56	0.30	0.50
LAR	Larissa	−15.2	0.83	0.36	0.54
VOL	Volos	−11.9	0.73	0.30	0.54
Mean (Greece)		**−3.8**	**1.08**	**0.49**	**0.65**

Table 7. Statistical metrics for SO_2 mean daily concentrations ($\mu g/m^3$) for each monitoring site over Thessaloniki, Greece (for d03 domain, 2×2 km^2) and the rest of Greece (for d02 domain, 6×6 km^2) for the cold period of 2015 (January–April, October–December) for the on-line SCN.

Site Name	Location in Greece	MB	Fac2	R	IOA
Thissio	Athens	18.7	2.0	0.33	0.49
Martiou	Thessaloniki	1.3	1.3	0.61	0.56
Malakopi	Thessaloniki	0.9	1.3	0.36	0.54
Mean (Greece)		**6.9**	**1.5**	**0.43**	**0.53**

The evaluation of the air quality modeling system using the "on-line" heating emissions reveals satisfactory model performance. In particular, on average, for all sites over Greece, the statistical analysis shows good model performance for O_3 concentrations, with Fac2 being close to 1 while the IOA is equal to 0.76. CO concentrations are generally underestimated by the model, with Fac2 equal to 0.85 and an MB of -0.17 mg/m^3, averaged over all stations studied. An underestimation of NO and NO_2 concentrations is shown in most of the monitoring sites, while the IOA ranges from 0.53 to 0.80. Better model performance for PM10 concentration levels is shown for the area of Athens, with an IOA up to 0.85, while the model underestimated PM10 levels in smaller urban centers (i.e., Larissa, Volos, Ioannina), mainly due to the fact that the grid cells of 6×6 km^2 where the corresponding monitoring sites are located include also non-urban areas, leading to lower mean PM levels. For the Thessaloniki area, the IOA is estimated up to 0.67, with a Fac2 ranging from 0.87 to 1.17, indicating satisfactory model performance for PM10 levels.

Figure 7 illustrates the daily variation in the observed and simulated air quality levels during the cold period of the year at different monitoring sites over Greece. A criterion has been used regarding the selection of monitoring sites presented in Figure 7 based on the completion of measurement data (i.e., monitoring sites for which measurement data were available for at least the 90% of the study period). Regarding daily PM10 observed concentrations levels presented in Figure 7, an upper threshold of 200 $\mu g/m^3$ has been applied since these values are considered as dust transport events and therefore are not related to central heating emissions, while these events seem to have been underestimated by the model. Good agreement between observed and simulated CO concentrations, on a daily basis, during the cold period of the year is shown for Thissio station, Athens (Figure 7a), revealing good modeling performance in terms of heating emissions since CO is emitted substantially from biomass burning while Thissio station is located 500 m away from the road network, limiting the impact of road transport emissions. Satisfactory agreement on the daily variation in the simulated NO concentrations with the observed ones was observed, with an underestimation of modeled NO levels in December. The daily variation in PM10 levels is well captured by the model, with the exception of dust transport events, where an underestimation is found (in Figure S1, additional plots with the daily variation in PM10 levels for other monitoring sites for which full observed timeseries were available are presented). Similarly, for SO_2, mean daily simulated values are in agreement with observations for the majority of days.

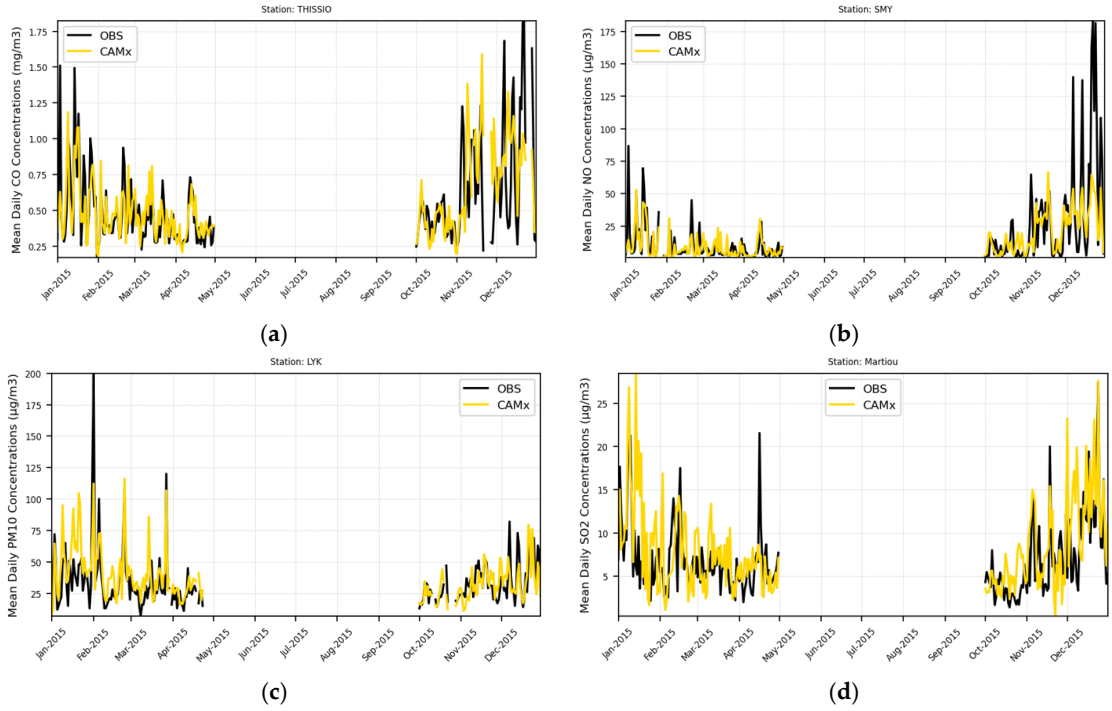


Figure 7. Mean daily (**a**) CO, (**b**) NO, (**c**) PM10 and (**d**) SO_2 concentrations of measurement and simulated data at different monitoring sites over Greece for the cold period of 2015 (January–April, October–December) for the on-line SCN.

A comparison of the correlation coefficient and the Index of Agreement between the on-line SCN and static SCN was made for different pollutants and for all monitoring sites (Figure 8). The comparison showed highly improved values of R, for the on-line SCN, for all the pollutants in the different monitoring sites except for PM10 in five out of the twelve sites, for which a slight improvement is shown for the static SCN mainly due to the slight overestimation of PM10 concentrations in the on-line SCN on specific days where the simulated air temperature was low. Regarding IOA, a general improvement is identified for the on-line SCN for almost all the cases, while the IOA for NO seems to be almost the same for the two scenarios, with a slight improvement for the on-line SCN.

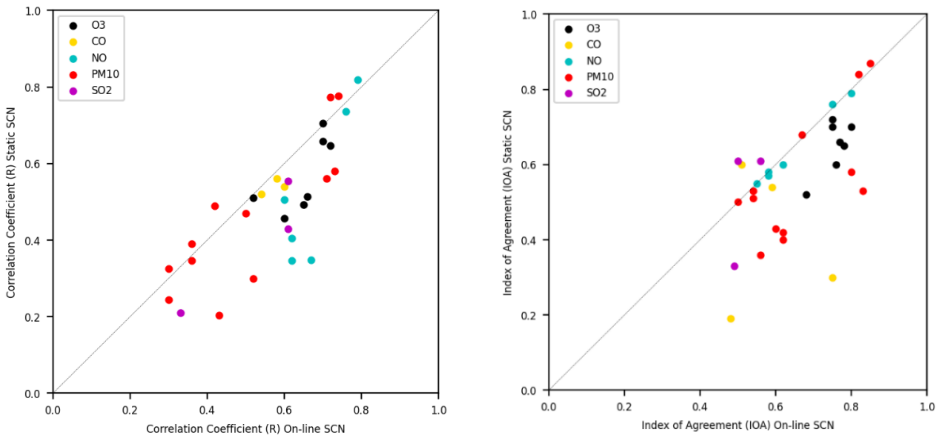


Figure 8. Comparison of the estimated (**a**) correlation coefficient (R) and (**b**) between on-line SCN and static SCN for O_3, CO, NO, PM10 and SO_2 concentrations at the different monitoring sites studied for the cold period of 2015 (January–April, October–December).

Figure 9 presents a comparison of the mean monthly variation in air pollutant and particle levels between observations, on-line SCN and static SCN simulations. It should be noted that, for the zero monthly values shown in Figure 9, there were no available observed data. It seems that the use of static emissions tends to underestimate air quality levels mainly in winter months. In particular, an improvement in the mean monthly CO levels for the on-line SCN is identified for all months. Better agreement for the monthly variation in NO levels is also shown between observed and on-line SCN simulated levels compared to static SCN. For PM10 levels, an improvement in simulated air quality levels is observed for most of the months in Nea Smyrni (SMY) station in the on-line SCN. Mean SO_2 concentrations are also improved in the on-line SCN compared to static SCN for Martiou station, in Thessaloniki, mainly for most of the months, while an overestimation of SO_2 concentrations is shown for the static SCN.

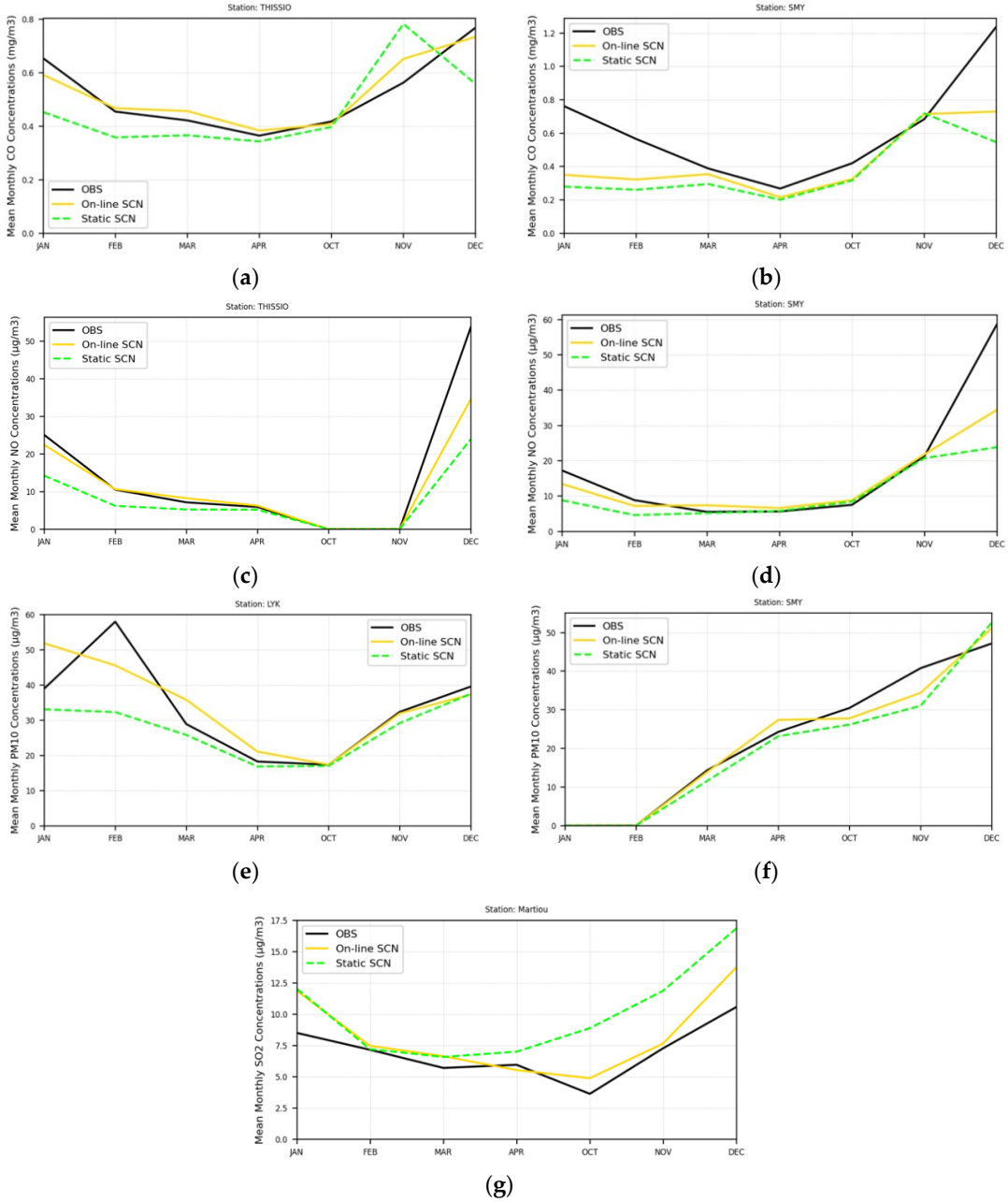


Figure 9. Comparison of CO (**a**,**b**), NO (**c**,**d**), PM10 (**e**,**f**) and SO_2 (**g**) mean monthly concentrations between observed and simulated data for on-line SCN and static SCN scenarios at different monitoring sites over Greece for the cold period of 2015 (January–April, October–December).

4. Conclusions

This study presented a new "on-line" heating emissions modeling system integrated with the air quality modeling system WRF-CAMx. The emissions modeling system calculates heating emissions from oil, natural gas and biomass burning (wood, biomass) over Greece based on the simulated Heating Degree Days (HDD) of the WRF model.

It was estimated that, for the cold period of the year, heating was the major contributor to PM10 and PM2.5 emissions by 47% and 60%, respectively, and the second highest contributor to CO emissions. The monthly variation in heating emissions followed the monthly variation in the simulated air temperature, leading to the highest emissions in January and February. Moreover, it was identified that on-line heating emissions led to lower emissions in spring/autumn months by up to −65% in comparison with winter months of the cold period, in contrast with the static monthly profiles usually used in emission inventories, where smaller differences (~−15 to −30%) are presented.

The modeling system was evaluated through the comparison of measurement and simulated pollution data over Greece for the cold period of 2015, applying the air quality modeling system for two different scenarios: the on-line SCN (based on WRF meteorology) and static SCN (based on static temporal profiles). The evaluation of the model for the on-line SCN showed overall satisfactory performance, while the model captures well the mean day-to-day variation in air quality levels in most of the cases. IOA and R values are identified to be improved in the on-line SCN for most of the pollutants and monitoring sites relative to that of the static SCN. Moreover, better agreement with observations is shown for the mean monthly variation in all pollutants studied for the on-line SCN compared to that of static SCN.

The current emissions modeling system has been integrated with the operational air quality modeling system of the project KASTOM (Innovative System for Air Quality Monitoring & Forecasting) of the Operational Program Competitiveness, Entrepreneurship and Innovation. Thus, future scientific effort will focus on the evaluation of the forecast air quality data in order to validate the emissions modeling system for different study years. Moreover, future research work may allow socioeconomic indicators to be introduced directly by the user so as to account for changes in near-future social or financial statistics such as population migration, unemployment rate, etc.

Supplementary Materials: The following supporting information can be downloaded at: https://www.mdpi.com/article/10.3390/atmos13040568/s1, Table S1: Description of the selected meteorological monitoring sites in Greece; Table S2: Description of the selected air pollution monitoring sites in Greece; Figure S1: Mean daily PM10 concentrations of measurement and simulated data at (a) AGP, (b) Dimarxeio, (c) Malakopi and (d) Martiou stations for the cold period of 2015 (January–April, October–December) for the On-line SCN.

Author Contributions: Conceptualization, N.L.; Methodology, N.L. and S.K.; Supervision, D.M.; Validation, N.L., D.P. and D.A.; Visualization, N.L.; Writing—original draft, N.L.; Writing—review and editing, N.L., A.P., D.K.P. and D.M. All authors have read and agreed to the published version of the manuscript.

Funding: This research has been cofinanced by the European Union and Greek national funds through the Operational Program Competitiveness, Entrepreneurship, and Innovation (call RESEARCH–CREATE–INNOVATE, project code T1EDK-01697).

Institutional Review Board Statement: Not applicable.

Informed Consent Statement: Not applicable.

Data Availability Statement: Simulated data can be provided upon request.

Acknowledgments: The authors would like to acknowledge the support provided by the Scientific Computing Center at the Aristotle University of Thessaloniki throughout the progress of this research work. We thank also P. Tzoumaka, A. Kelessis and E. Gerasopoulos for the measurement data availability. We thank also The Netherlands Organization for providing the anthropogenic emission database of CAMS-REGv.2.2 and the anthropogenic dust resuspension emission data.

Conflicts of Interest: The authors declare no conflict of interest.

References

1. European Environment Agency (EEA). *Air Quality in Europe-2018 Report (No. 12)*; European Environment Agency: København, Denmark, 2018; ISSN 1977-8449. Available online: https://www.eea.europa.eu/publications/air-quality-in-europe-2016 (accessed on 1 March 2021).
2. Markakis, K.; Poupkou, A.; Melas, D.; Tzoumaka, P.; Petrakakis, M. A Computational Approach Based on GIS Technology for the Development of an Anthropogenic Emission Inventory of Gaseous Pollutants in Greece. *Water Air Soil Pollut.* **2010**, *207*, 157–180. [CrossRef]
3. Moussiopoulos, N.; Vlachokostas, C.; Tsilingiridis, G.; Douros, I.; Hourdakis, E.; Naneris, C.; Sidiropoulos, C. Air quality status in Greater Thessaloniki Area and the emission reductions needed for attaining the EU air quality legislation. *Sci. Total Environ.* **2009**, *407*, 1268–1285. [CrossRef] [PubMed]
4. Panopoulou, A.; Liakakou, E.; Gros, V.; Sauvage, S.; Locoge, N.; Bonsang, B.; Psiloglou, B.E.; Gerasopoulos, E.; Mihalopoulos, N. Non-methane hydrocarbon variability in Athens during wintertime: The role of traffic and heating. *Atmos. Chem. Phys.* **2018**, *18*, 16139–16154. [CrossRef]
5. Bolling, A.K.; Pagels, J.; Yttri, K.E.; Barregard, L.; Sallsten, G.; Schwarze, E.P.; Boman, C. Health effects of residential wood smoke particles: The importance of combustion conditions and physicochemical particle properties. *Part. Fibre Toxicol.* **2009**, *6*, 29. [CrossRef] [PubMed]
6. Li, H.; You, S.; Zhang, H.; Zheng, W.; Zou, L. Analysis of the impacts of heating emissions on the environment and human health in North China. *J. Clean. Prod.* **2019**, *207*, 728–742. [CrossRef]
7. Sarigiannis, D.A.; Karakitsios, S.P.; Kermenidou, M.; Nikolaki, S.; Zikopoulos, D.; Semelidis, S.; Papagiannakis, A.; Tzimou, R. Total exposure to airborne particulate matter in cities: The effect of biomass combustion. *Sci. Total Environ.* **2014**, *493*, 795–805. [CrossRef]
8. Athanasopoulou, E.; Speyer, O.; Brunner, D.; Vogel, H.; Vogel, B.; Mihalopoulos, N.; Gerasopoulos, E. Changes in domestic heating fuel use in Greece: Effects on atmospheric chemistry and radiation. *Atmos. Chem. Phys.* **2017**, *17*, 10597–10618. [CrossRef]
9. Fameli, K.-M.; Assimakopoulos, V.D. The new open Flexible Emission Inventory for Greece and the Greater Athens Area (FEI-GREGAA): Account of pollutant sources and their importance from 2006 to 2012. *Atmos. Environ.* **2016**, *137*, 17–37. [CrossRef]
10. Kaskaoutis, D.G.; Grivas, G.; Theodosi, C.; Tsagkaraki, M.; Paraskevopoulou, D.; Stavroulas, I.; Liakakou, E.; Gkikas, A.; Hatzianastassiou, N.; Wu, C.; et al. Carbonaceous Aerosols in Contrasting Atmospheric Environments in Greek Cities: Evaluation of the EC-tracer Methods for Secondary Organic Carbon Estimation. *Atmosphere* **2020**, *11*, 161. [CrossRef]
11. Saffari, A.; Daher, N.; Samara, C.; Voutsa, D.; Kouras, A.; Manoli, E.; Karagkiozidou, O.; Vlachokostas, C.; Moussiopoulos, N.; Shafer, M.M.; et al. Increased Biomass Burning Due to the Economic Crisis in Greece and Its Adverse Impact on Wintertime Air Quality in Thessaloniki. *Environ. Sci. Technol.* **2013**, *47*, 13313–13320. [CrossRef]
12. Markakis, K.; Poupkou, A.; Melas, D.; Zerefos, C. A GIS based anthropogenic PM10 emission inventory for Greece. *Atmos. Pollut. Res.* **2010**, *1*, 71–81. [CrossRef]
13. Markakis, K.; Katragkou, E.; Poupkou, A.; Melas, D. MOSESS: A New Emission Model for the Compilation of Model-Ready Emission Inventories—Application in a Coal Mining Area in Northern Greece. *Environ. Model. Assess.* **2013**, *18*, 509–521. [CrossRef]
14. Skamarock, W.C.; Klemp, J.B.; Dudhia, J.; Gill, D.O.; Barker, D.M.; Duda, M.G.; Huang, X.Y.; Wang, W.; Powers, J.G. *A Description of the Advanced Research WRF Version 3*; U.S. National Center for Atmospheric Research: Boulder, CO, USA, 2008.
15. Solomou, E.S.; Pappa, A.; Kioutsioukis, I.; Poupkou, A.; Liora, N.; Kontos, S.; Melas, D. Analog ensemble technique to post-process WRF-CAMx ozone and particulate matter forecasts. *Atmos. Environ.* **2021**, *256*, 118439. [CrossRef]
16. Drosoglou, T.; Bais, A.F.; Zyrichidou, I.; Kouremeti, N.; Poupkou, A.; Liora, N.; Giannaros, C.; Koukouli, M.E.; Balis, D.; Melas, D. Comparisons of ground-based tropospheric NO_2 MAX-DOAS measurements to satellite observations with the aid of an air quality model over the Thessaloniki area, Greece. *Atmos. Chem. Phys.* **2017**, *17*, 5829–5849. [CrossRef]
17. Liora, N.; Poupkou, A.; Giannaros, T.M.; Kakosimos, K.E.; Stein, O.; Melas, D. Impacts of natural emission sources on particle pollution levels in Europe. *Atmos. Environ.* **2016**, *137*, 171–185. [CrossRef]
18. Liora, N.; Markakis, K.; Poupkou, A.; Giannaros, T.M.; Melas, D. The natural emissions model (NEMO): Description, application and model evaluation. *Atmos. Environ.* **2015**, *122*, 493–504. [CrossRef]
19. Marecal, V.; Peuch, V.H.; Andersson, C.; Andersson, S.; Arteta, J.; Beekmann, M.; Benedictow, A.; Bergstrom, R.; Bessagnet, B.; Cansado, A.; et al. A regional air quality forecasting system over Europe: The MACC-II daily ensemble production. *Geosci. Model Dev.* **2015**, *8*, 2777–2813. [CrossRef]
20. Zyrichidou, I.; Balis, D.; Koukouli, M.E.; Drosoglou, T.; Bais, A.; Gratsea, M.; Gerasopoulos, E.; Liora, N.; Poupkou, A.; Giannaros, C.; et al. Adverse results of the economic crisis: A study on the emergence of enhanced formaldehyde (HCHO) levels seen from satellites over Greek urban sites. *Atmos. Res.* **2019**, *224*, 42–51. [CrossRef]
21. Poupkou, A.; Markakis, K.; Liora, N.; Giannaros, T.M.; Zanis, P.; Im, U.; Daskalakis, N.; Myriokefalitakis, S.; Kaiser, J.W.; Melas, D.; et al. A modeling study of the impact of the 2007 Greek forest fires on the gaseous pollutant levels in the Eastern Mediterranean. *Atmos. Res.* **2014**, *149*, 1–17. [CrossRef]

22. Kontos, S.; Liora, N.; Giannaros, C.; Kakosimos, K.; Poupkou, A.; Melas, D. Modeling natural dust emissions in the central Middle East: Parameterizations and sensitivity. *Atmos. Environ.* **2018**, *190*, 294–307. [CrossRef]
23. Kontos, S.; Kakosimos, K.; Liora, N.; Poupkou, A.; Melas, D. Towards a regional dust modeling system in the central Middle East: Evaluation, uncertainties and recommendations. *Atmos. Environ.* **2021**, *246*, 118160. [CrossRef]
24. ENVIRON. *User's Guide CAMx Comprehensive Air Quality Model with Extensions*, 6.5th ed.; Ramboll US Corporation: Novato, CA, USA, 2018.
25. ECMWF, European Centre for Medium-Range Weather Forecasts. Available online: https://www.ecmwf.int/ (accessed on 1 November 2019).
26. Inness, A.; Blechschmidt, A.M.; Bouarar, I.; Chabrillat, S.; Crepulja, M.; Engelen, R.J.; Eskes, H.; Flemming, J.; Gaudel, A.; Hendrick, F.; et al. Data assimilation of satellite-retrieved ozone, carbon monoxide and nitrogen dioxide with ECMWF's Composition-IFS. *Atmos. Chem. Phys.* **2015**, *15*, 5275–5303. [CrossRef]
27. Granier, C.; Darras, S.; van der Gon, H.D.; Jana, D.; Elguindi, N.; Bo, G.; Michael, G.; Marc, G.; Jalkanen, J.P.; Kuenen, J.; et al. *The Copernicus Atmosphere Monitoring Service Global and Regional Emissions (April 2019 Version), Copernicus Atmosphere Monitoring Service (CAMS) Report*; Laboratoire d'Aérologie: Toulouse, France, 2019.
28. Crippa, M.; Guizzardi, D.; Muntean, M.; Schaaf, E.; Dentener, F.; van Aardenne, J.A.; Monni, S.; Doering, U.; Olivier, J.G.J.; Pagliari, V.; et al. Gridded emissions of air pollutants for the period 1970–2012 within EDGAR v4.3.2. *Earth Syst. Sci. Data* **2018**, *10*, 1987–2013. [CrossRef]
29. Open Source Geospatial Foundation. *GDAL/OGR Geospatial Data Abstraction Software Library*; Open Source Geospatial Foundation: Beaverton, OR, USA, 2020.
30. Schulzweida, U. CDO User Guide, Version 1.9.9. 2020. Available online: https://code.mpimet.mpg.de/ (accessed on 1 November 2020).
31. Schaap, M.; Manders, A.M.M.; Hendriks, E.C.J.; Cnossen, J.M.; Segers, A.J.S.; Denier van der Gon, H.A.C.; Jozwicka, M. *Regional Modelling of Particulate Matter for The Netherlands*; Research Program on Particulate Matter; PBL: Bilthoven, The Netherlands, 2009.
32. EMEP/EEA. *Air Pollutant Emission Inventory Guidebook*; Publications Office of the European Union: Luxemburg, 2016.
33. EMISIA. COPERT, Version 5.2. 2019. Available online: https://www.emisia.com/utilities/copert/versions/ (accessed on 1 February 2019).
34. Argyriou, A.; Gaglia, A.; Daskalaki, E.; Zacharias, P.; Katsanos, D.; Kontogiannidis, S.; Ladopoulos, G.; Ladopoulos, I.T.O.T.E.E. *Technical Guidelines*, 3rd ed.; 20701-3/2010; Ministry for the Environment, Energy and Climate Change: Athens, Greece, 2014.
35. Fourtziou, L.; Liakakou, E.; Stavroulas, I.; Theodosi, C.; Zarmpas, P.; Psiloglou, B.; Sciare, J.; Maggos, T.; Bairachtari, K.; Bougiatioti, A.; et al. Multi-tracer approach to characterize domestic wood burning in Athens (Greece) during wintertime. *Atmos. Environ.* **2017**, *148*, 89–101. [CrossRef]
36. Gratsea, M.; Liakakou, E.; Mihalopoulos, N.; Adamopoulos, A.; Tsilibari, E.; Gerasopoulos, E. The combined effect of reduced fossil fuel consumption and increasing biomass combustion on Athens' air quality, as inferred from long term CO measurements. *Sci. Total Environ.* **2017**, *592*, 115–123. [CrossRef]
37. Kalogridis, A.-C.; Vratolis, S.; Liakakou, E.; Gerasopoulos, E.; Mihalopoulos, N.; Eleftheriadis, K. Assessment of wood burning versus fossil fuel contribution to wintertime black carbon and carbon monoxide concentrations in Athens, Greece. *Atmos. Chem. Phys.* **2018**, *18*, 10219–10236. [CrossRef]
38. El.STAT. Manufacturing Products (PRODCOM Survey): Production and Sales/2015. 2015. Available online: https://www.statistics.gr/el/statistics/-/publication/SIN06/2015 (accessed on 1 January 2020).
39. El.STAT. 2011 Population-Housing Census. 2011. Available online: https://www.statistics.gr/en/2011-census-pop-hous (accessed on 1 January 2020).